

## Pseudorapidity distribution of shower particles in heavy ion induced interactions in nuclear emulsion at high energy

F. H. Liu<sup>1,\*</sup> and Yu. A. Panebratsev<sup>2,†</sup>

<sup>1</sup>*Department of Physics, Shanxi Teachers University, Linfen, Shanxi Province 041004, China*

<sup>2</sup>*Laboratory of High Energies, Joint Institute for Nuclear Research, Dubna, Moscow Region 141980, Russia*

(Received 26 August 1998)

The pseudorapidity distribution of shower particles produced in nuclear emulsions in heavy ion induced interactions have been studied at high energies. The thermalized cylinder picture is successful in the description of the pseudorapidity distribution of shower particles in the accelerator energy regions available at present. The calculated results are in agreement with the experimental data of 3.7A, 14.6A, 60A, and 200A GeV O-AgBr, 14.6A GeV Si-AgBr, 200A GeV S-AgBr, and 10.6A GeV Au-Em (emulsion) interactions. [S0556-2813(99)05102-X]

PACS number(s): 25.75.Dw, 24.10.Pa

The study of heavy ion interactions at high energies is an important field of modern particle and nuclear physics. On the one hand, the quark-gluon plasma (quark matter) predicted by various theories has been searched for in high energy heavy ion interactions. On the other hand, some properties obtained from nuclear reactions have been explained by the current knowledge of physics.

Under present experimental conditions, high energy heavy ion interactions are achieved via fixed target experiments. Hopes for improved experimental conditions are set on relativistic heavy ion colliders to be completed in the near future. Presently, however, by serving as a fixed target and detector, nuclear emulsions can capture an interaction event in its entirety and with a high resolution of particle tracks.

In nuclear emulsion experiments [1–5] the emission angles,  $\theta$ , of shower particles (relativistic singly charged particles) can be measured with great precision, and usually they are presented in terms of the pseudorapidity variable  $\eta = -\ln \tan(\theta/2)$ . The resulting distribution can often be described by a single Gaussian distribution [6–10]. Recently, however, the pseudorapidity distribution of shower particles produced in interactions of gold ions in nuclear emulsions at 10.6A GeV was found not to be described by a single Gaussian distribution. A long tail in the high  $\eta$  region contributed by projectile spectator protons has to be considered [7,11]. Especially for peripheral collisions, a two-peak structure is observed [11]. The EMU01 Collaboration used two Gaussian distributions, one for charged mesons and one for projectile spectator protons, to describe the pseudorapidity distribution of shower particles produced in 10.6A GeV Au-Em (emulsion) interactions.

In this paper, we shall study the pseudorapidity distribution of shower particles within the thermalized cylinder picture. A simple formula can give a good description of the pseudorapidity distribution in both cases of one and two Gaussians.

Let us consider the simplest pictures of the one-dimensional string model [12] and the fireball model [13]. In a high energy nucleon-nucleon collision, a string is formed consisting of two endpoints acting as energy reservoirs and the interior with constant energy per length. Because of the asymmetry of the mechanism, the string will break into many substrings along the direction of the incident beam. The distribution length of substrings will define the width of the pseudorapidity distribution. According to the fireball model, the incident nucleon penetrates through the target nucleon, then a firestreak is formed along the direction of the incident beam. The length of the firestreak will define the width of pseudorapidity distribution. In high energy nucleus-nucleus collisions, many strings or firestreaks are formed along the incident direction. Finally, a thermalized cylinder [14] is formed because of these strings or firestreaks mix in the transverse direction.

In the laboratory reference frame, we assume that the thermalized cylinder formed in nucleus-nucleus collisions is in the rapidity range  $[y_{\min}, y_{\max}]$ . The emission points with the same rapidity,  $y_x$ , in the thermalized cylinder form a cross section (emission plane) in the rapidity space. For the thermalized cylinder, the initial extension of the nuclei is not important because of Lorentz contraction.

Under the assumption that the particles are emitted isotropically in the rest frame of the emission plane, we know that the pseudorapidity distribution of the particles produced in the emission plane with rapidity  $y_x$  in the laboratory reference frame is

$$f(\eta, y_x) = \frac{1}{2 \cosh^2(\eta - y_x)}. \quad (1)$$

The pseudorapidity distribution measured in final state is contributed by the whole thermalized cylinder and the projectile and target spectators. We can consider both the integral of Eq. (1) and the contributions of the leading projectile and target protons in participants and spectators and obtain the pseudorapidity density distribution

\*Now at Laboratory of High Energies, JINR, Dubna, Moscow Region 141980, Russia. Electronic address: liu@sunhe.jinr.ru; liufh@dns.sjtc.edu.cn; liufh@dns.sxtu.edu.cn

†Electronic address: panebrat@sunhe.jinr.ru

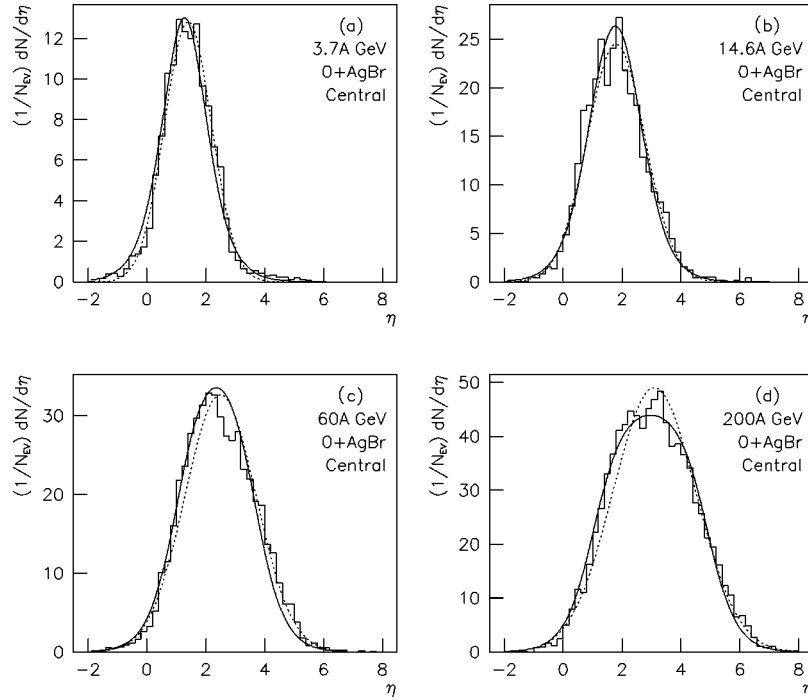


FIG. 1. Pseudorapidity distributions of shower particles for central interactions of  $^{16}\text{O}$  with AgBr at 3.7A (a), 14.6A (b), 60A (c), and 200A (d) GeV. The histograms are experimental data of Ref. [10]. The dotted and solid curves are results of the Gaussian distribution and thermalized cylinder picture, respectively.

$$\rho(\eta) = \frac{\langle N \rangle - \alpha N_{PP} - N_{PS}}{y_{\max} - y_{\min}} \int_{y_{\min}}^{y_{\max}} f(\eta, y_x) dy_x + \alpha N_{PP} f(\eta, y_{\max}) + N_{PS} f(\eta, y_{PS}), \quad (2)$$

where  $\langle N \rangle$  denotes the mean number of shower particles,  $N_{PP}$  and  $N_{PS}$  denote the proton numbers of projectile participant and spectator, respectively,  $\alpha$  is the probability of projectile participant proton appearing as a leading particle, and  $y_{PS}$  is the mean rapidity of projectile spectator protons. The contributions of leading target participant and spectator are not included in Eq. (2) due to the nonrelativity of leading target protons in fixed target emulsion experiments in the accelerator energy region at present. While, the contributions of nonleading projectile and target participant protons are included in  $\langle N \rangle$  in the first term of Eq. (2).

The string picture which we invoke to justify the model would imply that  $y_{\min} \approx y_{\text{target}} + \Delta y$  and  $y_{\max} \approx y_{\text{projectile}} - \Delta y$ , where  $y_{\text{target}}$ ,  $y_{\text{projectile}}$ , and  $\Delta y$  denote the target rapidity, the projectile rapidity and the average rapidity shift suffered in a collision, respectively. For the purpose of convenience, we shall obtain  $y_{\min}$  and  $y_{\max}$  by fitting experimental data in this paper.

The parameter  $\alpha$  in Eq. (2) is introduced to describe the probability of projectile participant proton appearing as a leading particle. Then,  $1 - \alpha$  denotes the probability of projectile participant proton appearing as a nonleading particle in the same thermalized cylinder as pions. The nonleading protons and the pions distribute in the cylinder from  $y_{\min}$  to  $y_{\max}$  and are subjected to the same flow velocity. The NA35 Collaboration has measured the rapidity distribution of protons in central  $^{32}\text{S}$ -S collisions at 200A GeV by “+−” method [15]. It is shown that the protons distribute in a wide rapidity range from  $y_{\min}$  to  $y_{\max}$ . At the same time, two

peaks are observed at  $y_{\min}$  and  $y_{\max}$ . We can say that the projectile participant protons have a probability  $\alpha$  appearing as leading protons at  $y_{\max}$  and a probability  $1 - \alpha$  appearing as nonleading protons in the range from  $y_{\min}$  to  $y_{\max}$ . The target participant protons have also a probability  $\alpha$  appearing as leading protons at  $y_{\min}$  and a probability  $1 - \alpha$  appearing as nonleading protons in the range from  $y_{\min}$  to  $y_{\max}$ . As a raw estimate, we take  $\alpha = 0.5$  in the analyses of emulsion data in this paper.

In the case of relative large projectile comparing with target, we need all three terms in Eq. (2) to describe the pseudorapidity distribution of shower particles. In the case of relative small projectile comparing with target, we need only the first and the second terms to describe the pseudorapidity distribution due to  $N_{PS}$  being zero or small value. In very peripheral collisions of relative small projectile and relative large target, maybe we need all three terms in Eq. (2) to describe the pseudorapidity distribution.

The EMU01 Collaboration has measured systematically the pseudorapidity distributions of shower particles produced in interactions of  $^{16}\text{O}$ ,  $^{28}\text{Si}$ , and  $^{32}\text{S}$  with AgBr at high energies [10], where AgBr are two of main components in nuclear emulsion. Figure 1 presents the pseudorapidity distributions of shower particles produced in central interactions of  $^{16}\text{O}$  with AgBr at 3.7A (a), 14.6A (b), 60A (c), and 200A (d) GeV. The histograms are experimental results of the EMU01 Collaboration [10]. For the purpose of comparison, the results of one Gaussian distribution [10] are given in the figure by dotted curves. The solid curves in Fig. 1 are results of Eq. (2) with only the first and the second terms. We obtain the values of  $y_{\min}$  and  $y_{\max}$  by fitting the experimental data, and obtain the values of  $\langle N \rangle$  by normalization condition. In central collisions,  $N_{PP}$  is the proton number of projectile in the case of relative small projectile comparing with target. In

TABLE I. Values of various parameters used in Eq. (2).

Figure	$y_{\min}$	$y_{\max}$	$y_{PS}$	$\langle N \rangle^a$	$\alpha$	$N_{PP}$	$N_{PS}$	$\chi^2/\text{DOF}$
1(a)	1.05	1.45		26.5	0.5	8.0		0.207
1(b)	1.05	2.40		61.5	0.5	8.0		0.494
1(c)	1.05	3.55		101.2	0.5	8.0		0.441
1(d)	1.05	4.80		175.9	0.5	8.0		0.347
2(a)	1.05	2.40		89.2	0.5	14.0		0.673
2(b)	1.05	4.80		339.4	0.5	16.0		0.795
3(a)	1.25	2.95	4.6	10.1	0.5	1.6	6.2	0.041
3(b)	1.25	2.95	4.6	28.4	0.5	8.0	15.5	0.086
3(c)	1.25	2.95	4.6	114.8	0.5	50.0	25.0	0.280
3(d)	1.25	2.95	4.6	334.7	0.5	70.0	9.0	0.751

<sup>a</sup>From the normalization condition.

the fit by Eq. (2), nonempty bins of the experimental data in the pseudorapidity region  $-2 < \eta < 8$  were used. The values of all parameters in thermalized cylinder picture are given in Table I. Both the Gaussian distribution and thermalized cylinder picture give a good description of the experimental data.

Figures 2(a) and 2(b) present the pseudorapidity distributions of shower particles produced in central interactions of  $^{28}\text{Si}$  with AgBr at 14.6A GeV and  $^{32}\text{S}$  with AgBr at 200A GeV, respectively. The histograms are experimental results of the EMU01 Collaboration [10]. The dotted and solid curves are results of one Gaussian distribution [10] and Eq. (2) with only the first two terms, respectively. Except  $\langle N \rangle$  and  $N_{PP}$ , other parameter values for Figs. 2(a) and 2(b) are the same as those for Figs. 1(b) and 1(d), respectively. In central collisions,  $N_{PP}$  is the proton number of projectile in the case of relative small projectile comparing with target. The parameter values used in Fig. 2 and the values of  $\chi^2/\text{DOF}$  are given in Table I. We notice that both the Gaussian distribution and thermalized cylinder picture give a good description of the experimental data.

Figure 3 presents the pseudorapidity distributions of shower particles produced in interactions of gold ions in nuclear emulsion at 10.6A GeV for four kinds of centralities: very peripheral (a), peripheral (b), semicentral (c), and very central (d). The circles are experimental results of the EMU01 Collaboration [11]. The dotted and solid curves are results of two Gaussian distributions [11] and Eq. (2), respectively. In the calculation of thermalized cylinder picture,

we obtain  $y_{\min}$ ,  $y_{\max}$ ,  $y_{PS}$ ,  $N_{PP}$ , and  $N_{PS}$  by fitting the experimental data. The values of  $\langle N \rangle$  in Eq. (2) are obtained by normalization condition. In the fit, the nonempty bins of the experimental data in the pseudorapidity region  $-2 < \eta < 8$  were used. The parameter values used in Fig. 3 and the values of  $\chi^2/\text{DOF}$  are given in Table I. In the case of relative large projectile comparing with target, both the two-Gaussian distribution and thermalized cylinder picture give a good description of the experimental data.

From Figs. 1 and 2, in the case of relative small projectile and a given collision centrality and target, one can see that the values of  $y_{\min}$  do not depend on the incident energy and projectile. The values of  $y_{\max}$  increase with increasing incident energy and do not depend on the projectile. From Fig. 3, in the case of a given incident energy and interacting system, one can see that the values of  $y_{\min}$  and  $y_{\max}$  do not depend on collision centrality. There is a decrease in the contribution of projectile participant protons when passing from central to peripheral interactions.

In Table I, we have chosen the same  $y_{\min}$  for the first six cases due to the same target (AgBr) for these cases. At the same time, we have chosen the same  $y_{\min}$  and the same  $y_{\max}$  for the last four cases due to the same target (Em) and the same incident energy and projectile (10.6A GeV Au) for these cases. We have chosen different  $y_{\max}$  for the first four cases due to the different incident energies. We would like to say that these parameter values are good choices according to the values of  $\chi^2/\text{DOF}$ . Maybe, these parameter values are not the best choice. In fact, we can also get a good result if we change  $y_{\min}$  and  $y_{\max}$  by  $\pm 0.05$ . We have not found obvious difference in  $y_{\min}$  (or  $y_{\max}$ ) for different centralities. The value of  $\alpha$  is not sensitive to the pseudorapidity distribution of shower particles. The contribution of the second term in Eq. (2) is much smaller than that of the first one.

We have studied the pseudorapidity distribution of shower particles in 11.6A GeV/c Au-Ag interactions by the thermalized cylinder picture [16]. For the peripheral example,  $y_{\min}=1.3$ ,  $y_{\max}=3.0$ . For the central example,  $y_{\min}=1.2$ ,  $y_{\max}=2.9$ . We notice that the values of  $y_{\min}$  for the two examples approximate equal and the values of  $y_{\max}$  for the two examples approximate equal, too. We have also studied the pseudorapidity distribution of shower particles in 158A GeV/c Pb-Pb interactions by the thermalized cylinder picture [17]. For high multiplicity (central and semicentral) events,  $y_{\min}=0.8$ ,  $y_{\max}=5.0$ . For the highest multiplicity

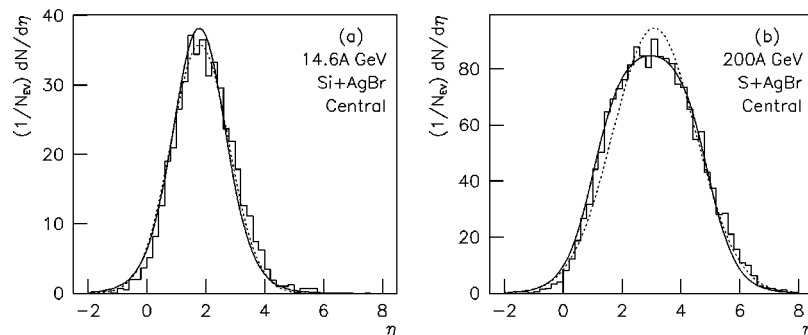


FIG. 2. Pseudorapidity distributions of shower particles for central interactions of  $^{28}\text{Si}$  with AgBr at 14.6A GeV (a) and  $^{32}\text{S}$  with AgBr at 200A GeV (b). The histograms are experimental data of Ref. [10]. The dotted and solid curves are results of the Gaussian distribution and thermalized cylinder picture, respectively.

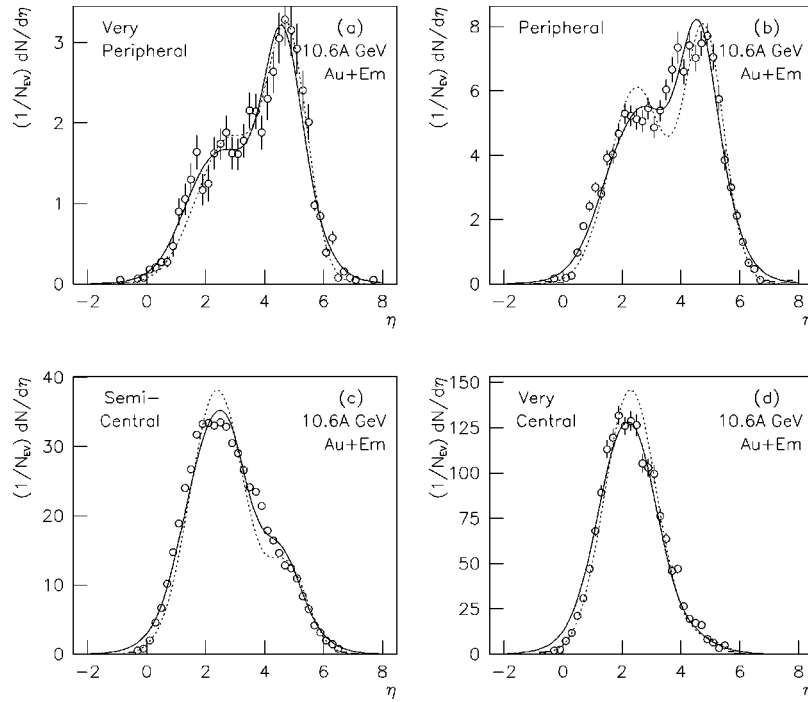


FIG. 3. Pseudorapidity distributions of shower particles in interactions of gold ions in nuclear emulsion at 10.6A GeV for four kinds of centralities: very peripheral (a), peripheral (b), semicentral (c), and very central (d). The circles are experimental data of Ref. [11]. The dotted and solid curves are results of the two-Gaussian distribution and thermalized cylinder picture, respectively.

(very central) event,  $y_{\min}=0.9$ ,  $y_{\max}=4.9$ . We see nearly equal  $y_{\min}$  and nearly equal  $y_{\max}$  for the two examples.

In conclusion, the thermalized cylinder picture is successful in the description of the pseudorapidity distribution of shower particles in the accelerator energy region at present. A simple formula can give a good description of the pseudorapidity distribution in both cases of one and two Gaussians. In the case of relative small projectile and a given collision centrality and target, the endpoint  $y_{\min}$  of the thermalized cylinder does not depend on the incident energy and projectile, but the endpoint  $y_{\max}$  of the thermalized cylinder increases with the incident energy and does not depend on the projectile. In the case of a given incident energy and interacting system, the endpoints  $y_{\min}$  and  $y_{\max}$  of the thermalized cylinder do not depend on collision centrality, but there is a decrease in the contribution of projectile participant protons when passing from central to peripheral interactions.

Our calculated results are in agreement with the experimental data in the present accelerator energy region. We shall be interested to test the thermalized cylinder picture by the pseudorapidity distribution of shower particles (relativistic singly charged particles) produced in heavy ion interactions at the Relativistic Heavy Ion Collider (RHIC) and the Large Hadron Collider (LHC) in the near future.

One of the authors (F.H.L.) gratefully acknowledges the support of the Laboratory of High Energies at the Joint Institute for Nuclear Research, Dubna, Russia. His work was also supported by the China State Education Department Foundation for Returned Overseas Scholars, Shanxi Provincial Foundation for Returned Overseas Scholars (Main Project), Shanxi Provincial Foundation for Leading Specialists in Science, and Shanxi Provincial Science Foundation for Young Specialists.

[1] M.I. Adamovich *et al.*, EMU01 Collaboration, Phys. Lett. B **262**, 371 (1991).  
 [2] P.L. Jain *et al.*, Phys. Rev. C **44**, 844 (1991).  
 [3] M. El-Nadi *et al.*, Nuovo Cimento A **108**, 809 (1995).  
 [4] D. Ghosh *et al.*, Nuovo Cimento A **103**, 423 (1990).  
 [5] D. Ghosh *et al.*, Nuovo Cimento A **110**, 565 (1997).  
 [6] H von Gersdorff *et al.*, Phys. Rev. C **39**, 1385 (1989).  
 [7] R. Holyński, Nucl. Phys. **A566**, 191c (1994), and references therein.  
 [8] F.H. Liu and J.F. Sun, Nuovo Cimento A **110**, 775 (1997).  
 [9] M.I. Adamovich *et al.*, EMU01 Collaboration, Phys. Rev. Lett. **69**, 745 (1992).  
 [10] M.I. Adamovich *et al.*, EMU01 Collaboration, Z. Phys. C **56**, 509 (1992).  
 [11] M.I. Adamovich *et al.*, EMU01 Collaboration, Phys. Lett. B **352**, 472 (1995).  
 [12] K. Werner, Phys. Rep. **232**, 87 (1995).  
 [13] G.D. Westfall *et al.*, Phys. Rev. Lett. **37**, 1202 (1976).  
 [14] Yu.M. Sinyukov, V.A. Averchenkov, and B. Lörst, Z. Phys. C **49**, 417 (1991).  
 [15] H. Ströbele, NA35 Collaboration, Nucl. Phys. **A525**, 59c (1991).  
 [16] F.H. Liu, Acta Phys. Sin. (Overseas Edition) **7**, 321 (1998).  
 [17] F.H. Liu and Yu.A. Panebratsev, Can. J. Phys. (in press).